Structural Investigation on Water-Induced Phase Transitions of Poly(ethylene imine). 1. Time-Resolved Infrared Spectral Measurements in the Hydration Process

Tomoko Hashida,[†] Kohji Tashiro,*[,†] Sadahito Aoshima,[†] and Yoshiaki Inaki[‡]

Department of Macromolecular Science, Graduate School of Science, Osaka University, Toyonaka, Osaka 560-0043, Japan; and Department of Material and Life Science, Graduate School of Engineering, Osaka University, Suita, Osaka 565-0871, Japan

Received December 18, 2001

ABSTRACT: Time-resolved infrared spectral measurements were made successfully for studying the microscopic mechanism of water-induced solid-state phase transitions of poly(ethylene imine) (PEI) in the hydration process at room temperature. The initial sample, obtained by cooling the melt under a dry atmosphere, showed the infrared spectra characteristic of the anhydrate phase consisting of doubly stranded helices. When this sample was exposed into an atmosphere of 100% relative humidity, the infrared spectra were found to change in a multistage mode from anhydrate to hemihydrate (molar ratio of ethylene imine unit/water = 1/0.5) to sesquihydrate (1/1.5) and to dihydrate (1/2), where the molecular chains in the latter three phases take the planar-zigzag all-trans conformation and form the complexes with water through the hydrogen bonds. The spectral measurements were made also for heavy water (D_2O) as well as light water (H_2O), and the quantitative analysis could be made more successfully for the former case, because the overlap of the polymer bands with water bands could be avoided due to the shift of the broad absorption bands of water molecules. A comparison was made for the strength of hydrogen bonds between PEI and PEI, PEI and water, and water and water. The infrared bands characteristic of the amorphous region could be detected in the frequency region of 1800−2500 cm^{-1}, the intensities of which were found to decrease in parallel to the crystal phase transition, indicating that some parts of the amorphous region can also crystallize into the hydrates in the hydration process.

Introduction

Different from commercially available poly(ethylene imine) [PEI, $-(CH_2CH_2NH)_n-$], which is a branched polymer and is almost amorphous, linear PEI exhibits the various kinds of crystalline phases when the sample is controlled under a humid atmosphere. Chatani et al. found that linear PEI shows multistage phase transitions between the anhydrate and various types of hydrate.[1−3] They carried out the X-ray structure analyses of these crystalline phases and discovered that the anhydrate consists of a parallel array of doubly stranded helices and the hydrates take the all-trans planar-zigzag chain conformation, as shown in Figure 1. The hydrates found so far are three types, all of which are the crystalline complexes between PEI and water molecules: hemihydrate with molar ratio between ethylene imine (EI) monomeric unit and water (EI/water = 1/0.5), sesquihydrate (EI/water = 1/1.5), and dihydrate (EI/water = 1/2). (In this paper these crystal phases will be named anhydrate (0), hemihydrate (0.5), sesquihydrate (1.5), and dihydrate (2.0) for simplicity.)

As seen in Figure 1b, by supplying water molecules into the dry state of PEI, the double helices are separated to a pair of single chains of all-trans conformation. What kinds of driving forces cause such a dramatic structural change? This structural change reminds us the change in DNA between doubly stranded and singly stranded chains and also the coupling of DNA with transfer RNA in the translation of gene information. Analysis of the complicated phase transitions of the PEI−water system may give us some important and useful information for understanding the mysterious genetic phenomenon from the microscopic level. Another interesting aspect of PEI is seen in the field of gene therapy. According to some reports,[4−8] PEI is attracting attention as a polymer vector, which is a kind of carrier to bring DNA molecules safely and effectively into a target position of cancer. In this case PEI is said to form a complex with DNA to protect DNA from being trapped by virus receptors. These descriptions about the formation of polymer−polymer complex including doubly stranded helices of PEI itself allow us to speculate that PEI has some characteristic features concerning the interactions with other polymer chains as well as with water molecules.

As a polymer with similar properties, we are aware of poly(ethylene oxide) (PEO, $-[CH_2CH_2O]_n-$), which has a chemical structure equivalent electronically to that of PEI. PEO can form many kinds of complexes with various kinds of ionic species and is easily dissolved in water.[9] These two polymers commonly show two types of chain conformation, T_2G-type helix and all-trans zigzag form in the solid state. (The torsional angles around C−C bonds of PEI helical chain are 13° according to the analysis by Chatani et al.,[3] which are quite near the cis conformation. However, here it is called the T_2G form in the first approximation.) PEO shows usually the helical conformation[10,11] but is transferred to the planar-zigzag conformation by applying a

[†] Graduate School of Science, Osaka University.
[‡] Graduate School of Engineering, Osaka University.

10.1021/ma012204l CCC: $22.00
Published on Web 04/20/2002

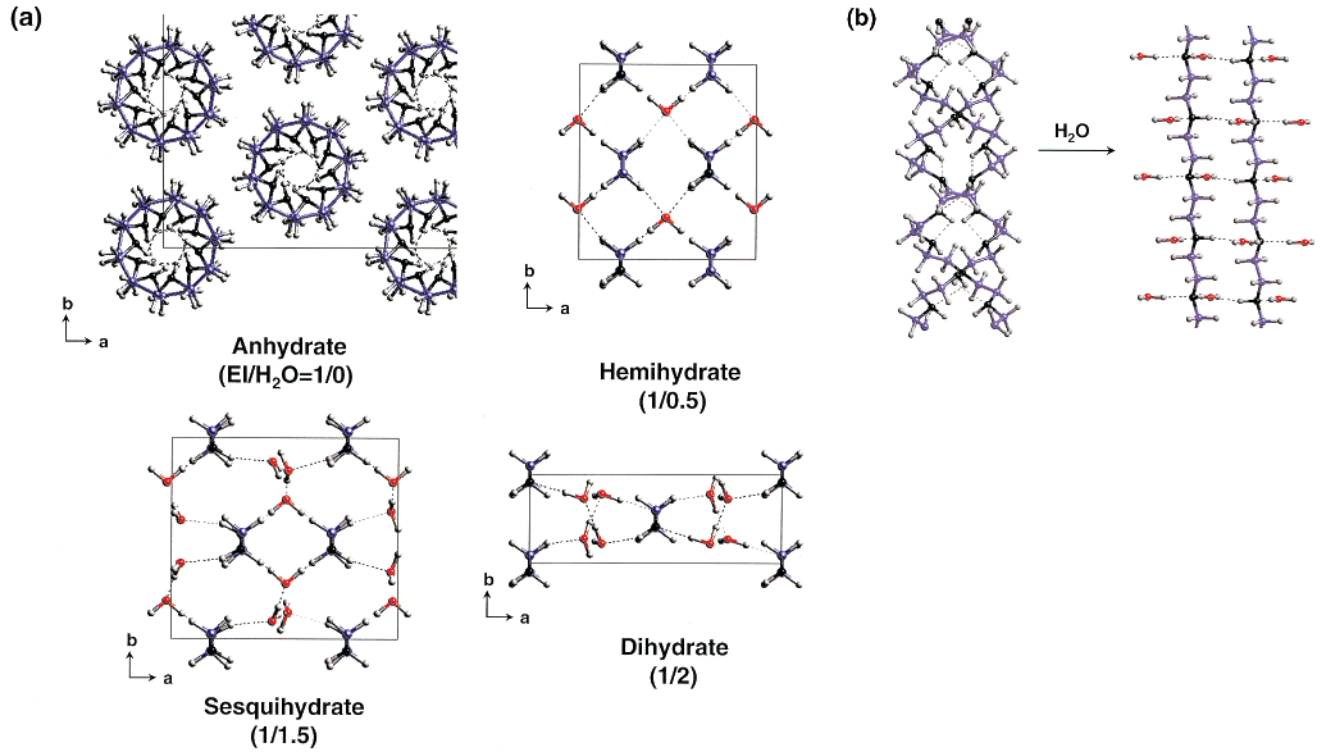

Figure 1. (a) Crystal structures of poly(ethylene imine). (b) Chain conformations of poly(ethylene imine) in the anhydrate (doubly stranded helices) and the hydrate (planar-zigzag form).

tensile force along the chain direction.[12,13] PEI shows the helical conformation in the "dried" solid state, and these helices are combined together to form a double strands, different from the case of PEO. The planar-zigzag form is realized by supplying water to this dried state. (We do not know whether PEI shows the trans-zigzag form under tensile stress, which is likely the case for PEO.) What kinds of factors control these crystal structures of T_2G-type helix and planar zigzag form of PEI and PEO?

To solve these various questions concerning the behavior of linear PEI, we need to reveal as basic information the details of the structural changes in the water-induced solid-state phase transition of PEI from the microscopic level. However, no detailed analysis has been made so far to clarify the transition mechanism between these various crystalline phases, although just one brief datum was reported about the change in X-ray diffraction profile measured during the hydration process.[3] In the present study, we have utilized vibrational spectroscopy as one of the most useful techniques for studying this area, which was expected to give us the microscopically viewed structural changes. Unfortunately, however, there has been no report at all about the vibrational spectral changes of PEI in the hydration process, nor even a report about any vibrational analysis of PEI. Then we were challenged to perform a series of vibrational spectroscopic studies of PEI including the time-resolved measurements of spectral changes in the transition process, the infrared band assignments of the various crystalline forms, and so on. In the present paper, we will describe the results on the time-resolved infrared spectral measurements of PEI in the hydration process, which will help us to obtain concrete images of transition behaviors of PEI before the detailed discussion of the transition mechanism.

Experimental Section

Samples. Linear PEI was prepared by alkaline hydrolysis of poly(*N*-acetyl ethylene imine)[14,15] which was supplied from Dow Chemicals Co. Ltd.

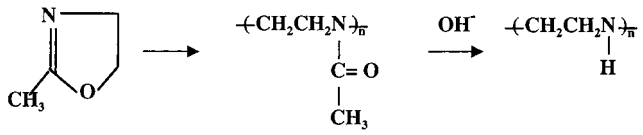

The molecular weight of PEI was about 500 000. The chemical structure was characterized by ^{1}H NMR spectroscopy. The measurement was made at 270 MHz for the $CDCl_3$ solution: $\delta_H = 2.7$ ppm (CH_2CH_2) and 1.58 ppm (NH). There was almost no signal for CH_3, indicating an almost perfect hydrolysis. Besides this, almost no peak was detected at about 2.5 ppm in the NMR spectra, which would have originated from the side branching structure of PEI. The films for infrared spectral measurements were prepared by pressing the molten sample between a pair of poly(tetrafluoroethylene) sheets, followed by drying up in vacuo for 7 days at 35 °C. Uniaxially oriented films were prepared by rolling the films at room temperature. The sample thickness was ca. 10 μm for the infrared spectral measurement and ca. 100 μm for the X-ray diffraction measurement.

Measurements. A film that was cooled from the mlet to room temperature was clamped into a metal holder and set in a homemade cell equipped with a water reservoir at the bottom (see Figure 2). For the windows of the infrared optical cell, oriented thin polyethylene films were used. This was because the KBr windows transparent to the infrared beam were easily made cloudy by water vapor and then the spectral background became worse. Of course KRS5, ZnSe, and so on are very popular for such a water system, but in the present experiment an oriented polyethylene film was conveniently used for the windows. The oriented polyethylene film shows only several bands in the infrared spectral region, and these bands have the perpendicular polarization with respect to the electric vector of the incident infrared beam. Therefore, by

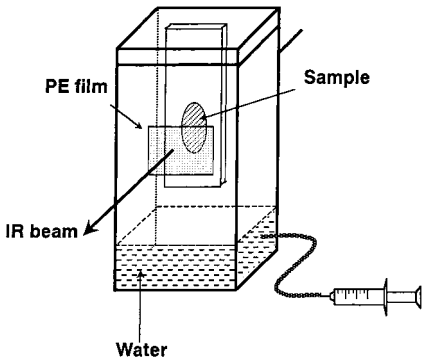

Figure 2. Optical cell for infrared spectral measurement under a constant relative humidity.

using an infrared beam with parallel electric vector, these bands do not appear in the infrared spectra. That is to say, an oriented polyethylene film can be used as an effective window for the water system as long as an infrared beam with parallel polarization is used. The thickness of the actually used polyethylene films was 10 μm. The time-resolved infrared measurement was performed by using a Bio-Rad FTS-60A FT-IR spectrometer equipped with an MCT detector at a resolution power of 2 cm^{-1}. The time interval between the successive spectra was 8 s.

For the X-ray diffraction experiments of the transmission mode, thin Mylar films were used for the cell windows. For the measurement of the X-ray diffraction of reflection mode, a sample of ca. 1 mm thickness was used. For such a thick sample, the phase transition occurred quite slowly over a few days even in an atmosphere of 100% relative humidity, and therefore, no special care was paid to the sample in the setting process. The time-resolved X-ray diffraction measurement of transmission mode was carried out by using a MAC Science DIP 1000 system combined with a CCD detector (C4880−20, Hamamatsu Photonics Co., Ltd.). The incident X-ray beam was a graphite-monochromatized Cu Kα line (λ = 1.5418 Å) from a MAC Science SRA18K rotating-anode-type X-ray generator. The reflection-mode measurement was carried out by using a Rigaku ROC diffractometer with a graphite-monochromatized Cu Kα line.

Results and Discussion

Infrared Spectral Changes in the Atmosphere of Light Water Vapor. The melt-cooled sample of PEI takes the crystalline form of anhydrate, as being checked by an X-ray diffraction measurement (see Figure 3). Infrared spectra were measured starting from this melt-cooled sample at a time interval of 8 s immediately after liquid water was injected into the optical cell (Figure 2). Strictly speaking, it will take some time for water molecules to fill the room of this cell. However, because of the small size of this cell, the starting time was defined as the moment of injecting liquid water into the cell. Parts a−c of Figure 4 show the time dependence of the thus measured infrared spectra of the melt-cooled PEI sample. The spectra obtained at 0 s are those of the anhydrate (0). As the time passed, these bands decreased in intensity and new bands appeared and increased (and then decreased) in intensity. These newly observed bands are considered to come from the bands characteristic of the hydrates with zigzag conformations. The broad bands are also observed to increase the intensity in the frequency regions 400−1000, 1600−1800, and 3000−3600 cm^{-1}, which are due to the vibrational modes of absorbed water. Among many bands observed in Figure 4, however, the bands useful for the quantitative analysis are quite limited. Some of them overlap with broad water

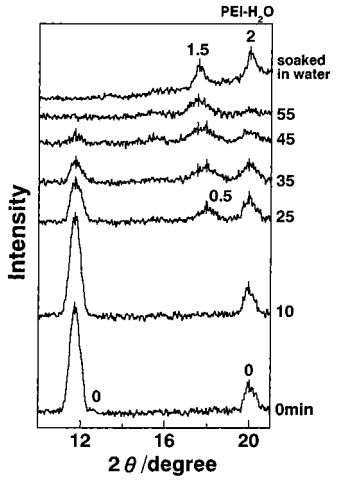

Figure 3. Time dependence of X-ray diffraction profile measured for poly(ethylene imine) at room temperature in the hydration process.

bands severely, and some other bands are observed at almost the same positions with each other. However, the following behavior may be described for several bands which are typical for anhydrate and hydrates. The band at 880 cm^{-1}, for example, decreased in intensity in the early stage of hydration. As the water band at 1650 cm^{-1} increased in intensity, the band at 876 cm^{-1} increased the intensity and then the 918 cm^{-1} band increased the intensity a little later than it. The band at 882 cm^{-1} could be assigned to that of anhydrate (0). The bands at 876 and 918 cm^{-1} might be of the hemihydrate (0.5) and sesquihydrate (1.5) or dihydrate (2.0). But, a definite assignment of the 876 and 918 cm^{-1} bands was difficult at this stage.

Infrared Spectral Changes in the Atmosphere of Heavy Water Vapor. Then we tried to use heavy water (D_2O) instead of light water (H_2O) with the expectation that the broad water bands might be shifted to lower frequency side and many bands which were hidden by these broad bands should be revealed. Parts a−c of Figure 5 show the thus measured infrared spectra after injection of D_2O liquid into an optical cell. In Figure 6 a comparison is made for the spectra between the cases of light and heavy waters in the frequency region of 450−1000 cm^{-1}. Figure 7 shows the time dependence of various bands found out of these spectra in the frequency region of 800−600 cm^{-1}, which had been hidden by broad water bands as long as H_2O was used in the experiment. In Figure 7 the intensity of the water band at 1200 cm^{-1} is also plotted. From the order of appearance and disappearance of these new bands, we could reasonably assign them to the four kinds of crystal phases: the band at 800 cm^{-1} to anhydrate (0), the band at 681 cm^{-1} to hemihydrate (0.5), the band at 660 cm^{-1} to sesquihydrate (1.5), and the band at 723 cm^{-1} to dihydrate (2.0).

Figure 8a shows the infrared spectra in the frequency region 1800−2500 cm^{-1}. Usually we do not pay almost any attention to such a frequency region because it corresponds to the overtone and/or combination modes of the normal vibrations. However, we were able to find that the band at 1903 cm^{-1} originated from the amorphous region. This band increased in intensity in the molten state of the sample, as seen in Figure 8b. This band is important since the intensity was found to decrease in parallel to an increment of the water band around 2200 cm^{-1} (Figure 8a). Therefore, we may say

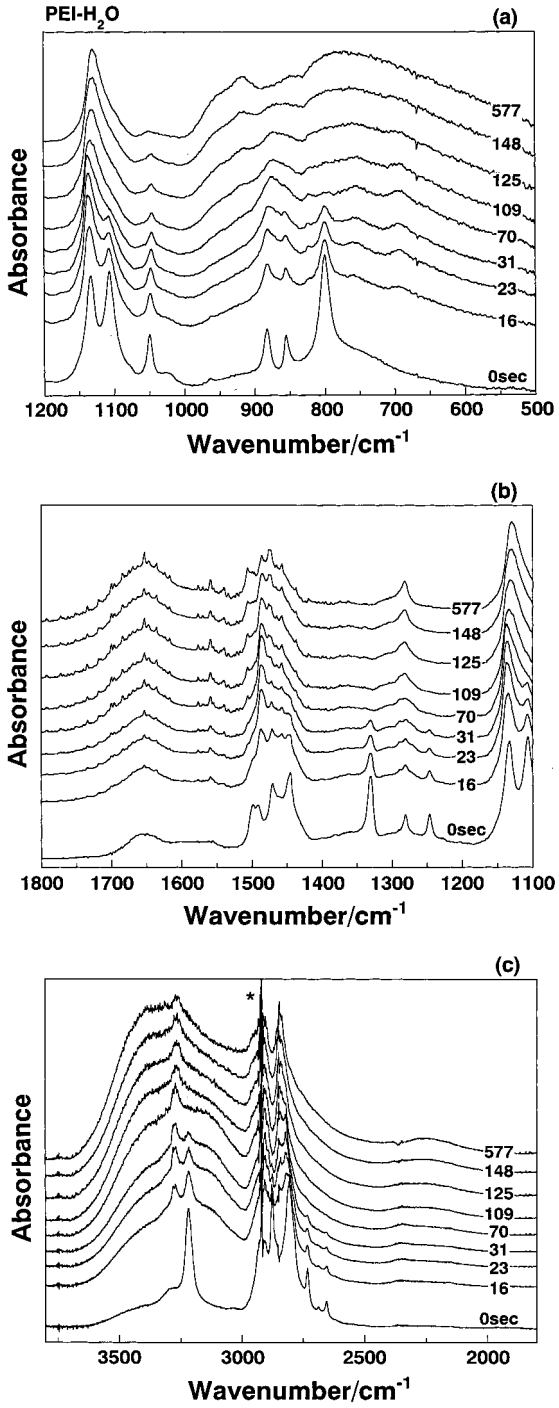

Figure 4. Time dependence of infrared spectra measured for poly(ethylene imine) at room temperature in the hydration process using light water. An asterisk indicates traces of bands from polyethylene used as window films.

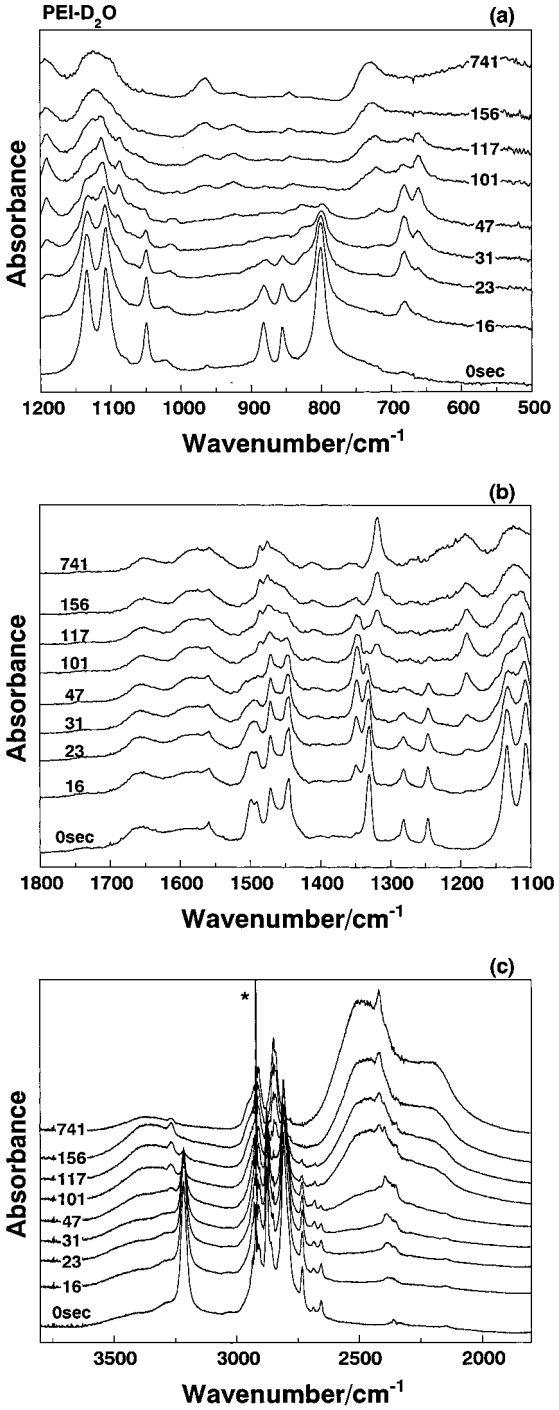

Figure 5. Time dependence of infrared spectra measured for poly(ethylene imine) at room temperature in the hydration process using heavy water. An asterisk indicates traces of bands from polyethylene used as window films.

that not only the crystalline phase of anhydrate but also the amorphous phase is considered to experience the transition to the hydrates by injecting water into the dry sample. The hydration-induced structural regularization in the amorphous region will be reported in more detail in a near future. If the whole region of the amorphous phase is changed to the crystalline hydrates, the sample might become almost purely crystalline state. However, the actual case was not so perfect, although the sample becomes rather brittle due to an increment of crystallinity. This may be because of the existence of chain entanglements, for example, which will suppress the smooth change of the randomly entangled amorphous chain segments into the fully extended zigzag form.

Polarized Infrared Spectra of Anhydrate and Hydrates. Although the infrared bands characteristic of various crystal phases could be identified quite well as mentioned above, it is more useful to have the polarized infrared spectra of oriented samples, because many overlapped bands might be separated by changing the polarization direction of the incident infrared beam. Figure 9 shows the time dependence of polarized infrared spectra of an oriented PEI sample in the D_2O

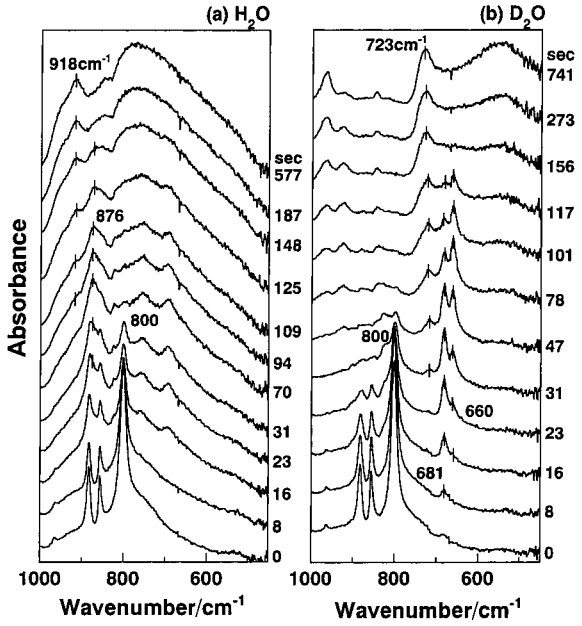

Figure 6. Comparison of infrared spectral changes of poly(ethylene imine) in the hydration process by using (a) light water and (b) heavy water.

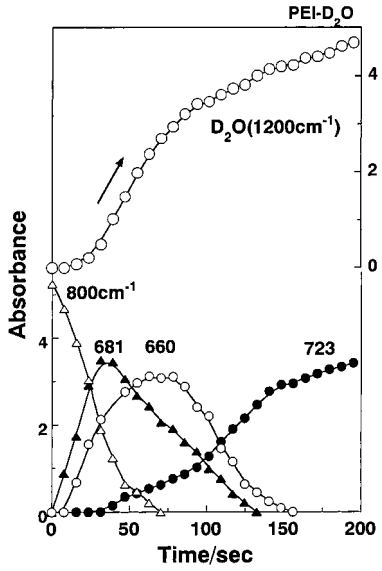

Figure 7. Time dependence of integrated intensity of various infrared bands of poly(ethylene imine) measured in the hydration process at room temperature in the atmosphere of heavy water vapor.

atmosphere, where the oriented sample was prepared by rolling the unoriented film at room temperature followed by drying up for a long time. The spectra keep high degree of polarization character or high order of chain orientation even after the transformation of the anhydrate (0) to the dihydrate (2.0) through hydration. Some of the infrared bands intrinsic of each crystalline phase are listed in Table 1, which will be useful for the further discussion of the transition mechanism. The detailed assignment of these bands to vibrational modes should be made on the basis of the normal-mode analysis and will be reported in a separate paper.

Relative Strength of Hydrogen Bonds. Figure 10 shows the infrared spectra in the frequency region 2000−3700 cm^{-1} which were taken in the D_2O atmosphere. The bands around 2200 and 2500 cm^{-1} are assigned to the OD stretching modes of heavy water.

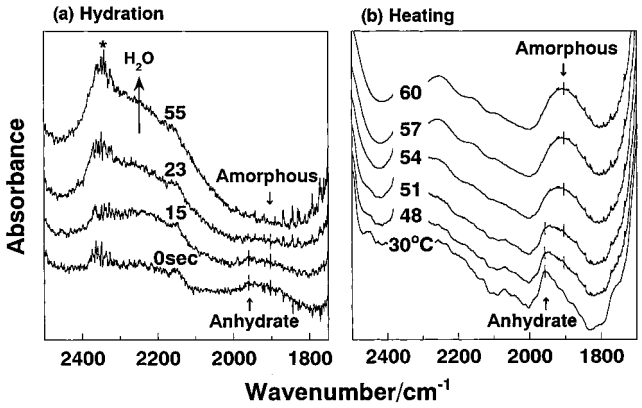

Figure 8. (a) Time dependence of infrared spectra in the frequency region of 1800−2500 cm^{-1}. An asterisk indicates the bands of CO_2 gas in the atmosphere. (b) Temperature dependence of infrared spectra in the same region. The band at 1958 cm^{-1} comes from the anhydrate and disappears by absorbing water (a) or by being heated above the melting point of ca. 60 °C (b). In part b, the band at 1903 cm^{-1} increases in intensity above the melting point, being assignable to the amorphous phase.

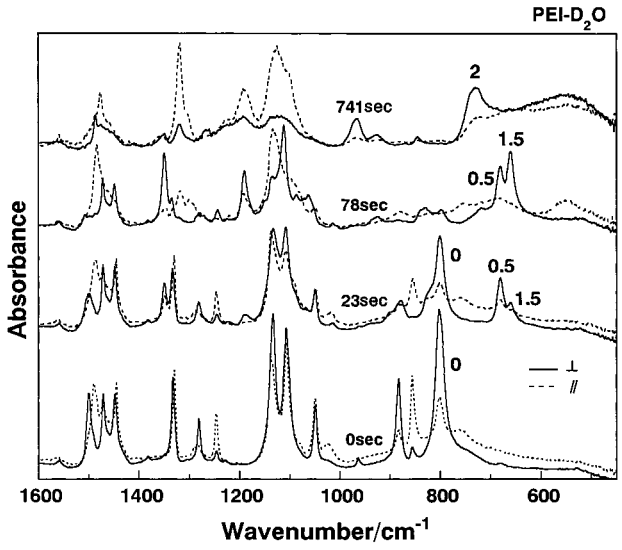

Figure 9. Time dependence of polarized infrared spectra of oriented poly(ethylene imine): (—) electric vector of incident infrared beam perpendicular to the orientation direction; (---) electric vector of incident infrared beam parallel to the orientation direction.

By absorption of D_2O, an exchange between H and D species occurred in NH groups and the ND stretching bands could be detected in the frequency region of 2400 cm^{-1}. Since the exchange between H and D was not always perfect, the NH stretching band of the anhydrate (0) can be also observed at 3220 cm^{-1}. The three bands are observed to change their relative intensity with increasing water content. The broad bands in the region of 2354−2400 cm^{-1} may be due to the ND stretching modes of hemihydrate (0.5). Then a sharp band appeared at 2396 cm^{-1}, the ND stretching mode of sesquihydrate (1.5). The band at 2418 cm^{-1} appearing in a later stage of hydration may come from the dihydrate (2.0). The band observed at 3266 cm^{-1} increased in intensity and could be assigned to NH stretching mode of sesqui- or dihydrate, judging from the intensity change.

The vibrational frequency of ND (and NH) stretching mode is higher in the order of anhydrate (0) < hemihydrate (0.5) < sesquihydrate (1.5) < dihydrate (2.0).

Table 1. Infrared Bands Characteristic of Anhydrate and Hydrates of Poly(ethylene imine)

	IR bands/ cm^{-1}	polarization[a]	modes[b]
		(a) H_2O	
anhydrate	800	⊥	
(EI/H_2O = 1/0)	856	∥	r(CH_2) + r(NH) + r(OH)
	883	⊥	
	1246	∥	
	1281	⊥	
	1291	∥	ω(CH_2) + t(CH_2)
	1330	∥	
	1333	⊥	
	3214	∥	ν(NH)
	3220	⊥	
hemihydrate	876	⊥	r(CH_2) + r(NH) + r(OH)
(1/0.5)	1289	∥	ω(CH_2) + t(CH_2)
	3267	⊥	ν(NH)
	3278	∥	
sesquihydrate	876	⊥	r(CH_2) + r(NH) + r(OH)
(1/1.5)	1289	∥	ω(CH_2) + t(CH_2)
dihydrate	918	⊥	r(CH_2) + r(NH) + r(OH)
(1/2)	1282	∥	ω(CH_2) + t(CH_2)
		(b) D_2O	
hemihydrate	681	⊥	r(CH_2) + r(ND) + r(OD)
(PEI/D_2O = 1/0.5)	1350	⊥	ω(CH_2) + t(CH_2)
	2358	⊥	
	2360	∥	ν(ND)
	2377	∥	
	2383	⊥	
sesquihydrate	660	⊥	r(CH_2) + r(ND) + r(OD)
(1/1.5)	1350	⊥	ω(CH_2) + t(CH_2)
	2396	⊥	ν(ND)
dihydrate	723	⊥	r(CH_2) + r(ND) + r(OD)
(1/2)	1301	∥	ω(CH_2) + t(CH_2)
	1318	∥	
	2418	⊥	ν(ND)

[a] ∥ and ⊥ indicate that the electric vector of incident infrared beam is parallel and perpendicular to the chain direction, respectively. [b] Key: r, rocking mode; ω, wagging mode; t, twisting mode; ν, stretching mode.

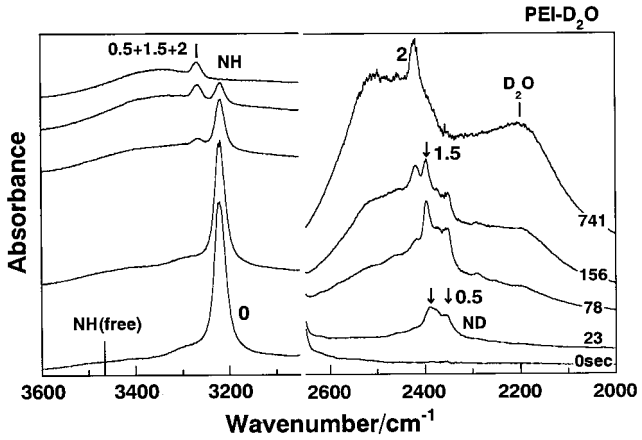

Figure 10. Time dependence of infrared spectra in the frequency region of stretching modes of N−H and O−H bonds (3600−3100 cm^{-1}) and of N−D and O−D bonds (2600−2000 cm^{-1}).

The anhydrate (0) was set in the lowest frequency position as judged from the spectral change observed in the NH stretching region of 3200 cm^{-1}: the band at 3220 cm^{-1} for the anhydrate (0) and the band at 3266 cm^{-1} for hydrates. It is also noticed that these NH and ND stretching bands are located at positions much lower than the freely isolated NH group, the vibrational frequency of which is about 3450 cm^{-1}. This indicates the strong interactions between the NH groups and between pairs of NH groups and water molecules. From the above-mentioned order in vibrational frequency, it may be reasonable to say that the NH···N hydrogen bond formed between a pair of doubly stranded helical chains in the anhydrate (0) is stronger than the NH··· O hydrogen bonds formed between PEI chains and surrounding water molecules. According to the X-ray structure analysis, the N···N distance is about 3.1 Å, which is comparable to twice the van der Waals radius of N atom (1.55 Å), and the N···N hydrogen bonds are considered to be very tight, as already discussed by Chatani et al.[2] As for the hydrates, the hydrogen-bond strength of N···O type is different among hydrates. The difference in vibrational frequency gives us the order of hemihydrate (0.5) > sesquihydrate (1.5) > dihydrate (2.0). This is also reasonable when the N···O interatomic distance is compared among them: 2.87−3.05 Å for hemihydrate (0.5), 2.93−2.96 Å for sesquihydrate (1.5), and 2.93 Å for dihydrate (2.0). (Of course the error in atomic position needs to be taken into account in this estimation.) It is also noticed that the OH···O type hydrogen bonds between water molecules show the different strength when compared with those of water liquid. Figure 11 compares the infrared spectra of PEI dihydrate (2.0) and pure D_2O taken at room temperature. The PEI−water complex (dihydrate (2.0)) shows mainly two broad bands around 2200 and 2450 cm^{-1}, while the neat water shows the broad peaks around 2400−2700 cm^{-1}, which may be assigned to symmetric and antisymmetric OD stretching modes of heavy water with various hydrogen bond strengths. The two main bands observed for the PEI−water complex might be also assigned to antisymmetric and symmetric OD stretching modes. The lower position of these bands suggests stronger OD···O hydrogen bonds between water molecules in the complex when compared with those in neat water.

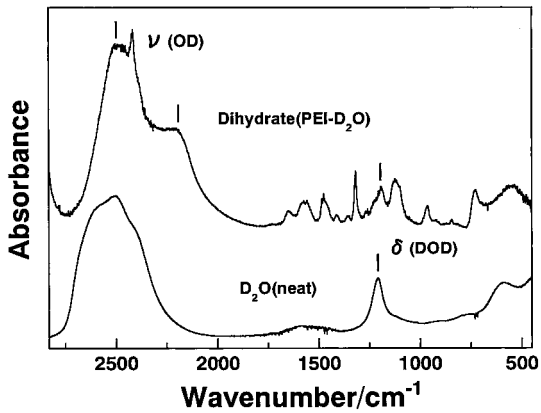

Figure 11. Comparison of infrared spectra in the frequency regions of O−D stretching mode (2600−2000 cm^{-1}) and DOD bending mode (1300−1100 cm^{-1}) between D_2O molecules in the poly(ethylene imine) hydrate and neat D_2O.

Conclusions

As described in the present paper, we have succeeded for the first time in measuring the infrared spectra of PEI and their changes in the hydration process starting from the anhydrate with doubly stranded helices to the PEI−water complexes of hemihydrate (0.5), sesquihydrate (1.5), and dihydrate (2.0). The infrared spectra of anhydrate are largely different from those of hydrates. It may be surprising to notice that the infrared spectra are remarkably different even among the hydrates despite their common chain conformations of planar-zigzag type. The difference in vibrational frequencies

may reflect sensitively the difference in the interaction between planar-zigzag PEI chains and surrounding water molecules. In other words, the PEI−water interaction affects largely the vibrational frequencies of internal modes of polymers. We notice also that the vibrational frequency of the N−H (N−D) stretching mode or the hydrogen bond strength is different among the crystal phases on the order of NH···N > NH···O (hemihydrate) > NH···O (sesquihydrate) > NH···O (dihydrate). Besides this, the water−water interactions in the complex are also different in strength from those observed in neat water liquid. The normal modes analysis will clarify these situations more concretely.

The infrared spectra were found to change at four stages from anhydrate (0) to hemihydrate (0.5) to sesquihydrate (1.5) and to dihydrate (2.0), being consistent with the observations made by the X-ray diffraction method. The infrared spectra showed us clearly and concretely the interactions between PEI and water molecules in the complexes. At the same time, the amorphous region was found to exhibit the partial change to the crystalline hydrates by absorbing water. This is also an important aspect in studying the morphological change in the higher order structure consisting of both the crystalline and amorphous phases.

The next stage of our research is to reveal the transition mechanism of four crystalline forms in the hydration process. In particular, the mechanism of structural change from doubly stranded helices to planar-zigzag chains may be one of the most difficult problems to solve. This is important also in relation with the biological problem of doubly stranded DNA chains. We believe the infrared spectral data obtained in the present study for these various crystal phases of PEI−water system will play a significant role in challenging such a difficult but important theme.

Acknowledgment. The authors wish to thank Dow Chemicals Co. Ltd. for their kind supply of poly(*N*-acetyl ethylene imine) sample. T.H. wishes to thank the Hayashi Memorial Foundation for Female Natural Scientists for their financial support.

References and Notes

(1) Chatani, Y.; Tadokoro, H.; Saegusa, T.; Ikeda, H. *Macromolecules* **1981**, *14*, 315.
(2) Chatani, Y.; Kobatake, T.; Tadokoro, H.; Tanaka, R. *Macromolecules* **1982**, *15*, 170.
(3) Chatani, Y.; Kobatake, T.; Tadokoro, H. *Macromolecules* **1983**, *16*, 199.
(4) Dick, C. R.; Ham, G. E. *J. Macromol. Sci. Chem.* **1970**, *A4*, 1301.
(5) Merlin, J.-L.; Dolivet, G.; Dubessy, C.; Festor, E.; Parache, R.-M.; Verneuil, L.; Erbacher, P.; Behr, J.-P.; Guillemin, F. *Cancer Gene Ther.* **2001**, *8*, 203.
(6) Goula, D.; Becker, N.; Lemkine, G. F.; Normandie, P.; Rodringues, J.; Mantero, S.; Levi, G. *Gene Ther.* **2000**, *7*, 499.
(7) Bragonzi, A.; Dina, G.; Villa, A.; Calori, G.; Biffi, A.; Bordignon, C.; Assael, B. M.; Conese, M. *Gene Ther.* **2000**, *7*, 1753.
(8) Bronich, T. K.; Nguyen, H. K.; Eisenberg, A.; Kabanov, A. *J. Am. Chem. Soc.* **2000**, *122*, 8339.
(9) Tadokoro, H. *Structure of Crystalline Polymers*; John Wiley and Sons: New York, 1979.
(10) Tadokoro, H.; Chatani, Y.; Yoshihara, T.; Tahara, S.; Murahashi, S. *Makromol. Chem.* **1964**, *73*, 109.
(11) Takahashi, Y.; Tadokoro, H. *Macromolecules* **1973**, *6*, 672.
(12) Takahashi, Y.; Sumita, I.; Tadokoro, H. *J. Polym. Sci., Polym. Phys. Ed.* **1973**, *11*, 2113.
(13) Tashiro, K.; Tadokoro, H. *Rep. Prog. Polym. Phys. Jpn.* **1978**, *21*, 417.
(14) Saegusa, T.; Ikeda, H.; Fujii, H. *Polym. J.* **1972**, *3*, 35.
(15) Saegusa, T.; Ikeda, H.; Fujii, H. *Macromolecules* **1972**, *5*, 359.

MA012204L